PHYSICAL REVIEW B **81**, 161306(R) (2010)

Free-electron-like Hall effect in high-mobility organic thin-film transistors

M. Yamagishi,[1] J. Soeda,[1] T. Uemura,[1] Y. Okada,[1] Y. Takatsuki,[1] T. Nishikawa,[1] Y. Nakazawa,[1] I. Doi,[2] K. Takimiya,[2] and J. Takeya[1,3,4,*]

[1]*Graduate School of Science, Osaka University, Toyonaka 560-0043, Japan*

[2]*Graduate School of Engineering, Hiroshima University, Higashi-Hiroshima, 739-8527, Japan*

[3]*ISIR, Osaka University, Ibaraki 567-0047, Japan*

[4]*PRESTO, Japan Science and Technology Agency, Kawaguchi 332-0012, Japan*

(Received 13 February 2010; revised manuscript received 29 March 2010; published 12 April 2010)

Gate-voltage-dependent Hall coefficient R_H is measured in high-mobility field-effect transistors of polycrystalline dinaphtho[2,3-b:2′,3′-f]thieno[3,2-b]thiophene films. The value of R_H evolves with density of accumulated charge q, precisely satisfying the free-electron formula $R_H=1/q$ near room temperature. The result indicates that the intrinsic charge transport inside the grains is bandlike in the vacuum-deposited high-mobility organic-semiconductor thin films that are of significant interest in industry. At lower temperatures, even Hall-effect mobility averaged over the whole polycrystalline film decreases due to the presence of carrier-trapping levels at the grain boundaries while the free-electron-like transport is preserved in the grains. With the separated description of the intergrain and the intragrain charge transport, it is demonstrated that the reduction in mobility with decreasing temperature often shown in organic thin-film transistors does not necessarily mean mere hopping transport.

DOI: 10.1103/PhysRevB.81.161306 PACS number(s): 73.61.Ph, 72.80.Le, 73.40.−c

Electronic charge transport in organic semiconductors is achieved by consecutively transferring charge from one π-conjugated molecule to another that is weakly interacted through van der Waals coupling. Though their transfer integral is typically one order of magnitude smaller than that in covalently bonded inorganic semiconductors, excellent self-assembling capability of the organic molecules enables them to condensate into a semiconductor film with moderate mobility μ as high as ~ 1 $\mathrm{cm}^2/\mathrm{V\,s}$ near room temperature. This process occurs even with relatively easy techniques such as solution coating or vapor deposition, providing the basis for the tremendous interest from industry. Indeed, it has been reported that μ of the polycrystalline organic thin-film transistors (OTFTs) in excess of that of amorphous-silicon films is attributed to "ordering" of the molecules.[1–4] As an ultimate performance of organic transistors, one order of magnitude higher values of μ are reported for rubrene single-crystal transistors, where molecular ordering is nearly perfect in the whole semiconductor channels.[5–7] Therefore, it is empirically conceived that extent of molecular ordering is an important factor to determine the carrier mobility, and hence the device performance. However, the mechanism that associates the microscopic molecular arrangement with macroscopic charge transport is yet to be elucidated.

For the charge dynamics in organic semiconductors, complexities originating from the "softness" are also to be taken into account, though it appends another attractiveness to the materials, providing mechanical flexibility for the use in large-area rollable displays, for example. Because of significant vibrational displacement of the molecules, the charge transport can be subjected to the nonadiabatic effect or "dynamical disorder" at room temperature.[8,9] Furthermore, the energy scale of their transfer integrals, which is on the order of 0.1 eV, is close to that of molecular reorganization upon ionization that could drive the system to self-localization of small polarons. In the semiconductor channels of organic transistors, interfacial states and dynamic coupling between the charge carriers and the gate-dielectric polarization can also be involved in the charge dynamics.[10] Because of these complexities, it is challenging to understand the fundamental charge-transport mechanisms in the OTFTs, which is also urgent because of the expectation for next-generation electronic devices. In order to experimentally elucidate the fundamental question whether the charge propagate diffusively by the band-transport mechanism or based on site-to-site hopping in the OTFTs, we employ Hall-effect measurement on organic transistors with high-mobility polycrystalline thin films, which is regarded to be also relevant for industrial applications.

Hall effect is viewed as linear response in charge flow to magnetic flux B, originated from an electromagnetic coupling between momentum $\hbar k$ of the charge q and vector potential A, which appears in the second term of the kinetic Hamiltonian $\frac{1}{2m^*}(\hbar k+qA)^2$. Therefore, the effect is grounded on electronic states that are spatially extended in sizable molecular sites so that the states can be defined with their wave vector k.[11] Within the free-electron approximation, the Hall coefficient $R_H \equiv V_H/(IB)$ equals to $1/Q$ with the charge density Q, where I represents the charge current. V_H is the Hall voltage in the direction perpendicular to both I and B. A correction parameter γ in the order of unity is multiplied to the right-hand side of the equation if elastic scattering is dominant.[12] If the charge is spatially localized and the transport is based on a site-to-site hopping (tunneling) between the electronic states described with their locations r's, on the other hand, there is no kinetic term to give rise to the Hall voltage.[13] Though interference between pairs of consecutive hopping processes results in finite Hall voltage, the value becomes much smaller than that for the free-electron-like carriers, as is demonstrated in amorphous-silicon TFTs.[14–16] Therefore, the measurement of Hall effect is useful to iden-

tify the fundamental transport mechanism in organic semiconductors.

Up to now, Hall-effect measurements were reported only for rubrene single-crystal transistors and pentacene thin-film transistors; the former showed typical free-electron values for R_H as a function of q (Refs. 17–19) whereas the latter showed significant deviation from $1/Q$.[20] Although also other probes indicate bandlike transport in rubrene single crystals,[21,22] the reason of the deviation in the pentacene thin film is not yet clear; it is experimentally difficult to prepare pentacene single-crystal transistors avoiding the effect of surface oxidization. In order to study the effect of the molecular ordering on microscopic carrier transport, it is particularly important to compare the transport in a single crystal independently grown from gas phase without any substrate and that in a grain of a thin film deposited on a substrate, using the same experimental setup. In the present experiment, we measured Hall effect and four-terminal conductivity of both single-crystal and granular thin-film transistors of dinaphtho[2,3-b:2′,3′-f]thieno[3,2-b]thiophene (DNTT) (Refs. 23 and 24) so that in-grain charge-transport mechanism, influence of the molecular ordering, and the effect of grain boundaries can be investigated for the same compound.

The single-crystal device (Sample SC) was prepared following the same method developed in our previous experiments for rubrene single-crystal transistors;[17,19] a thin platelet of the crystal was grown to the thickness of approximately 1 μm in a two-zone tube furnace by physical vapor transport and was attached electrostatically to a n^{++}-Si/SiO_2 substrate with source and drain electrodes already patterned with 20-nm-thick gold. The doped Si layer is used for the gate electrode and SiO_2 with the thickness of 500 nm forms the gate insulating layer, where the relative dielectric constant is 3.9 so that the gate capacitance C per area is evaluated to be 6.9 nF. Self-assembled monolayers (SAMs) are coated on the SiO_2 surface by depositing the vapor of decyltrichlorosilane.

In addition, two thin-film devices were vacuum deposited on the n^{++}-Si/SiO_2 substrates in different conditions; for Sample A, DNTT is deposited on n^{++}-Si/SiO_2 substrate with the SAMs in our best-tuned condition which usually realizes mobility exceeding 1 cm^2/V s, where temperature is actively controlled at the boat to keep the deposition rate at 0.5 Å/min. For Sample B, the film is deposited in one order of magnitude faster rate on the substrate without the SAMs. Gold is deposited to form top-contact electrodes of the source, drain, and additional pads to probe potentials in the channel. A laser-etching technique is employed for all the three samples to shape the channels for the Hall-bar configuration.

Figure 1(a) shows a top view of Sample A with the width W, length L, and distance l between the additional voltage-probing electrodes, which are 60 μm, 200 μm and 80 μm, respectively, for all the three samples. Atomic-force microscope (AFM) is used to characterize morphology of the thin-film samples as shown in Figs. 1(b) and 1(c) for Samples A and B, respectively, where apparent difference in the grain sizes is visible. As illustrated in Fig. 1(a), voltages V_1, V_2, and V_3 are measured at three different positions in the channel so that the two-dimensional (four-terminal) conductivity per square sheet $\sigma_\square$ $[=I/(V_2-V_1)l/W]$ and transverse voltage (V_3-V_1) are measured simultaneously as a function of gate voltage V_G. $\sigma_\square$ equals to the product of mobility and charge density q. Magnetic field is swept back and forth at least three times in the range from −10 to 10 T so that slowly drifting signal is subtracted to evaluate ΔV_H for the peak-to-peak magnetic field and R_H is evaluated by $\Delta V_H/(I\Delta B)$, where $\Delta B=20$ T.

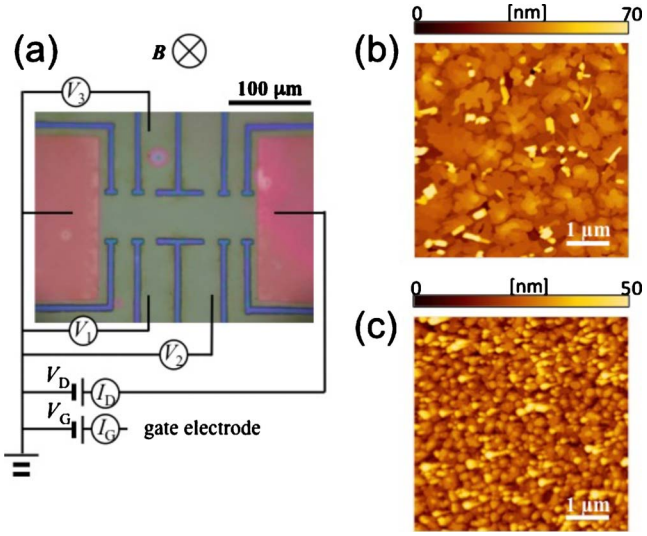

FIG. 1. (Color online) (a) Optical view of a DNTT thin-film transistor for the Hall-effect measurement. Schematic is also shown for the measurement of voltages at different positions in the channel. (b) AFM picture of the film deposited slowly at the rate of 0.5 Å/min (Sample A). (c) AFM picture of the film deposited at the much faster rate of 5 Å/min (Sample B).

Figure 2(a) shows the plot of the inverse Hall coefficient as a function of gate voltage for the single-crystal device (Sample SC) at room temperature. $1/R_H$ increases with negative V_G in accordance with the free-electron formula $1/R_H=|CV_G|$ within the accuracy of the measurement, pre-

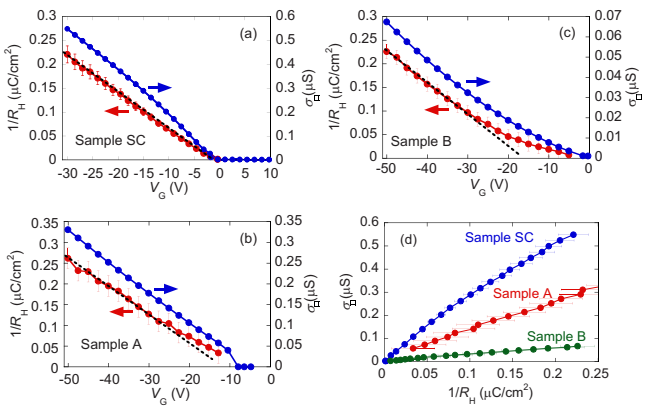

FIG. 2. (Color online) (a)–(c) Inverse Hall coefficient $1/R_H$ and sheet conductivity plotted as a function of gate voltage at 280 K. The slopes represented by the broken lines with the left-hand-side scale correspond to the capacitance of the gate insulator. (a), (b), and (c) are for Sample SC, Sample A, and Sample B, respectively. (d) Sheet conductivity vs inverse Hall coefficient at 280 K, plotted for Sample SC, Sample A, and Sample B.

senting a clear indication of the diffusive charge transport. The four-terminal sheet conductivity is plotted together, showing a monotonic evolution of $\sigma_{\square}$ with negative V_G due to the hole accumulation. We define field-effect mobility μ_{FET} on the four-terminal measurement $1/C \cdot \partial\sigma/\partial V_G$ and Hall-effect mobility μ_H as $R_H\sigma$. The single-crystal sample satisfies the free-electron formula in the Hall-effect measurement so that μ_{FET} is identical to μ_H. μ_{FET} is approximately 3 $cm^2/V\,s$, which reproduces the value of μ_{FET} in our previous experiment.[24] The whole results resemble those for high-mobility rubrene single crystals with $\mu_{FET} \sim 8$ $cm^2/V\,s$ at room temperature, which we reported previously.[19]

Figure 2(b) presents the plot for the device with the slowly deposited polycrystalline thin film (Sample A). Similarly as the result of the single-crystal device, $1/R_H$ increases with negative V_G following the slope defined by C, though threshold V_{th} is not negligible because of possible deep trap levels and/or dipoles at the interface. The result indicates that all the mobile charge is again diffusive with spatially extended electronic states. Due to the microscopic origin of the Hall effect, $1/R_H$ is not strongly influenced by the presence of grain boundaries as long as their intergrain electrical connection is fairly good, which is demonstrated in the present result itself. The measured Hall voltage appears as the summation of local Hall voltages generated at the grains in the direction perpendicular to the current. μ_{FET} is estimated to be approximately 1.2 $cm^2/V\,s$ using the result of the four-terminal sheet conductivity and is identical to μ_H. Note that the value is averaged over the whole channel including both intragrain and intergrain components in the DNTT thin film.

The plot for Sample B is shown in Fig. 2(c). For this sample, the increasing rate of $1/R_H$ with negative V_G is significantly smaller than that given by C in the region where $|V_G| < 30$ V. The result suggests that the carriers are not in motion all the time and that they are trapped at (shallow) interface states for a considerable period, as described by the multiple trap-and-release model.[25] The measured value of $1/R_H$ counts only time-averaged density of the moving charge.[18] The same behavior was reported for rubrene single-crystal transistors at temperatures slightly lower than room temperature.[18] With the application of higher V_G, however, the slope gradually approaches that defined by C, with the trapping sites being filled. μ_{FET} of 0.4 $cm^2/V\,s$ is obtained from the measurement of $\sigma_{\square}$ in the region of $|V_G| > 30$ V, which again includes the grain-boundary component. Since the difference in the results of the Hall-effect measurements for Samples A and B is attributed to properties inside the grains, we suspect that the shallow traps responsible for the multiple trap-and-release conduction would be in-grain molecular disorder. Indeed, x-ray diffraction experiments show a general tendency that thin films with smaller grains are of poorer crystallinity.[26] We are currently under way for high-intensity x-ray diffraction experiments to have more detailed description on the microscopic in-grain charge transport in conjunction with the molecular ordering.

In Fig. 2(d), $\sigma_{\square}$ is plotted against $1/R_H$, which can be regarded as the density of diffusive carriers affected by the electromagnetic force so that the slope gives Hall mobility μ_H. Note that this plot shows the value of μ_H more directly

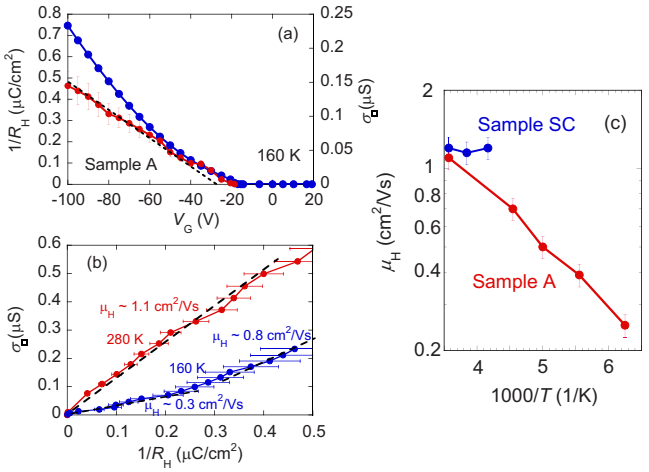

FIG. 3. (Color online) (a) Inverse Hall coefficient (red filled circles) and sheet conductivity (blue filled circles) plotted as a function of gate voltage for Sample A at 160 K. The slope represented by the broken line with the left-hand-side scale corresponds to the capacitance of the gate insulator. (b) Sheet conductivity vs inverse Hall coefficient in Sample A at 160 K. (c) Temperature dependence of Hall mobility in Sample A.

from the slope than the standard plots of $1/R_H$ vs CV_G and σ vs CV_G shown in Figs. 2(a)–2(c). $\mu_H = \mu_{FET}$ for Sample SC and Sample A while the equation is valid only with $|V_G| > 30$ V for Sample B; μ_H represents the carrier mobility of only well-mobile diffusive carriers while μ_{FET} includes the effect of (shallow) charge traps. The estimated mobility for Samples A and B still includes resistances at grain boundaries, which is partially responsible for their smaller values than that of Sample SC.

We measured the Hall effect also at lower temperatures for Sample A to have microscopic insight for the temperature dependence in high-mobility OTFTs, which is the most interested for application because temperature dependence of the mobility is often argued associated with the charge-transport mechanism. The result at 160 K is presented in Fig. 3(a). $1/R_H$ shows nearly linear regression as a function of V_G, which suggests that all the carriers transport like free electrons in Sample A even at 160 K. The $\sigma_{\square}$ vs $1/R_H$ plot shown in Fig. 3(b) indicates that the Hall mobility is smaller at a lower temperature in the region of low V_G. Although the concave curvature of the transfer characteristics qualitatively resemble those for Sample B at room temperature, the curvature in the $1/R_H$ vs V_G plot is different from that in Fig. 2(c), indicating that microscopic picture of the charge transport is different between the two cases.

Shown in Fig. 3(c) are μ_H measured similarly for Sample A in the low-V_G region and for Sample SC. The value of μ_H decreases monotonically with decreasing temperatures for Sample A while the temperature dependence is almost negligible down to 200 K for Sample SC (the crystal was damaged at 190 K due to different thermal-restriction rate in the Si substrate). Noting that the in-grain transport mechanism is bandlike as the result of the Hall-effect measurements for Sample A, it is not likely that local mobility in the grains decreases at low temperatures. Therefore, the temperature-dependent μ_H is attributed to an additional resistance at grain

boundaries; assuming in-gap trap levels at the boundaries, the temperature dependence is attributed to a thermally assisted process to release the trapped charges. As the result of the simultaneous measurements of Hall effect and four-probe conductivity, the plausible description of the charge transport in Sample A turned out to be a mixture of in-grain bandlike transport and temperature-dependent grain-boundary resistances. The picture is different from a simple argument that temperature dependence of decreasing mobility with decreasing temperature is an indication of mere hopping transport.

Finally, we would like to briefly remark on the mean-free path ℓ in the present semiconductor material as compared to that in rubrene crystal, based on μ measured in Sample SC. It was argued previously that ℓ in the rubrene crystal could be only a few times longer than the molecular distance at room temperature T within the simple nondegenerated two-dimensional electron-gas model, $\ell \sim \sqrt{2k_BTm^*}(\mu/e)$, if one assumes the effective mass m^* comparable to that of a free electron.[22] k_B is Boltzmann constant and e is the electron charge. Since it is difficult to assume even shorter ℓ for the diffusive charge transport, the difference in μ_{FET} between rubrene and DNTT would be attributed at least partially to the difference in m^*. Indeed, our simple calculation based on the extended Hückel molecular orbitals gives relatively small transfer integral of 79 meV for DNTT.[24] In order to fully understand dynamics of the carriers in these organic semiconductors, which seem to be on the verge of localization, direct measurement and/or more reliable calculation of m^*, more precise evaluation of ℓ are to be further proceeded toward establishment of the microscopic model of the charge transport in the "soft" crystals.

In conclusion, the simultaneous measurement of the Hall coefficient and four-terminal conductivity in the single-crystalline and polycrystalline samples of the DNTT field-effect transistors has provided separated description on the intragrain and intergrain charge transport. The electronic states are basically extended over molecules so that the band-like diffusive transport is realized, exhibiting the textbook-like free-electron Hall effect of $1/R_H$ identical to the amount of accumulated charge. The above feature is qualitatively same in independently grown single crystals and in a single domain of the polycrystalline film carefully deposited on a substrate, though the domains in lower-quality films include considerable charge-trap sites to slow down the charge motion. Grain boundaries affects to diminish the field-effect mobility measured for the whole polycrystalline films, giving a dominant contribution in further reducing mobility upon cooling. The fundamental charge transport does not rely on hopping in the high-mobility granular OTFT sample, even though mobility decreases with decreasing temperature.

We thank Nippon Kayaku Corporation for supplying DNTT used in the present study. We acknowledge that this study is financially supported by Industrial Technology Research Grant Programs from New Energy and Industrial Technology Development Organization (NEDO), Japan, and by a Grants-in-Aid for Scientific Research (Grants No. 17069003, No. 19360009, and No. 21108514) from the Ministry of Education, Culture, Sports, Science and Technology of Japan (MEXT).

*takeya@sanken.osaka-u.ac.jp

[1] J. E. Anthony *et al.*, J. Am. Chem. Soc. **123**, 9482 (2001).
[2] K. C. Dickey *et al.*, Adv. Mater. (Weinheim, Ger.) **18**, 1721 (2006).
[3] T. Izawa *et al.*, Adv. Mater. (Weinheim, Ger.) **20**, 3388 (2008).
[4] T. Uemura *et al.*, Appl. Phys. Express **2**, 111501 (2009).
[5] E. Menard *et al.*, Adv. Mater. (Weinheim, Ger.) **16**, 2097 (2004).
[6] J. Takeya *et al.*, Appl. Phys. Lett. **90**, 102120 (2007).
[7] C. Reese *et al.*, Appl. Phys. Lett. **89**, 202108 (2006).
[8] S. Fratini and S. Ciuchi, Phys. Rev. Lett. **103**, 266601 (2009).
[9] A. Troisi, D. L. Cheung, and D. Andrienko, Phys. Rev. Lett. **102**, 116602 (2009).
[10] I. N. Hulea *et al.*, Nature Mater. **5**, 982 (2006).
[11] See, e.g., H. Fukuyama *et al.*, Prog. Theor. Phys. **42**, 494 (1969).
[12] See, e.g., J. M. Ziman, *Electrons and Phonons* (Clarendon Press, Oxford, 1960), Chap. 12.
[13] M. Pope and C. Swenberg, *Electronic Processes in Organic Crystals and Polymers*, 2nd ed. (Oxford University Press, London, 1999), p. 374.
[14] L. Friedman, J. Non-Cryst. Solids **6**, 329 (1971).
[15] E. Arnold and J. M. Shannon, Solid State Commun. **18**, 1153 (1976).
[16] P. G. Le Comber *et al.*, Philos. Mag. **35**, 1173 (1977).
[17] J. Takeya *et al.*, Jpn. J. Appl. Phys. **44**, L1393 (2005).
[18] V. Podzorov, E. Menard, J. A. Rogers, and M. E. Gershenson, Phys. Rev. Lett. **95**, 226601 (2005).
[19] J. Takeya *et al.*, Phys. Rev. Lett. **98**, 196804 (2007).
[20] T. Sekitani *et al.*, Appl. Phys. Lett. **88**, 253508 (2006).
[21] O. Ostroverkhova *et al.*, Appl. Phys. Lett. **88**, 162101 (2006).
[22] Z. Q. Li, V. Podzorov, N. Sai, M. C. Martin, M. E. Gershenson, M. Di Ventra, and D. N. Basov, Phys. Rev. Lett. **99**, 016403 (2007).
[23] T. Yamamoto and K. Takimiya, J. Am. Chem. Soc. **129**, 2224 (2007).
[24] M. Uno *et al.*, Appl. Phys. Lett. **94**, 223308 (2009).
[25] G. Horowitz *et al.* (unpublished).
[26] T. J. Shin *et al.*, Chem. Mater. **19**, 5882 (2007).